Supporting Information

Light- and Temperature-dependent Dynamics of Chromophore and Protein Structural Changes in Bathy Phytochrome Agp2

Galaan Merga,[1] Maria Fernandez Lopez,[2] Paul Fischer,[1] Patrick Piwowarski,[1] Żaneta Nogacz,[1] Anastasia Kraskov,[2] David Buhrke,[2§] Francisco Velazquez Escobar,[2] Norbert Michael,[2] Friedrich Siebert,[3] Patrick Scheerer,[4] Franz Bartl,[1] and Peter Hildebrandt[2]*

[1] Humboldt Universität zu Berlin, Institut für Biologie, Biophysikalische Chemie, Invalidenstr. 42, D-10115 Berlin, Germany.

[2] Technische Universität Berlin, Institut für Chemie, Sekr. PC14, Straße des 17. Juni 135, D-10623 Berlin, Germany.

[3] Albert-Ludwigs-Universität Freiburg, Institut für Molekulare Medizin und Zellforschung, Sektion Biophysik, Hermann-Herderstr. 9, D-79104 Freiburg, Germany.

[4] Charité – Universitätsmedizin Berlin, corporate member of Freie Universität Berlin and Humboldt-Universität zu Berlin, Institute of Medical Physics and Biophysics, Group Protein X-ray Crystallography and Signal Transduction, Charitéplatz 1, D-10117 Berlin, Germany

[§] present address: University of Zürich, Department of Chemistry, Winterthurerstr. 190, CH-8057 Zürich, Switzerland

[*] Correspondence address: hildebrandt@chem.tu-berlin.de

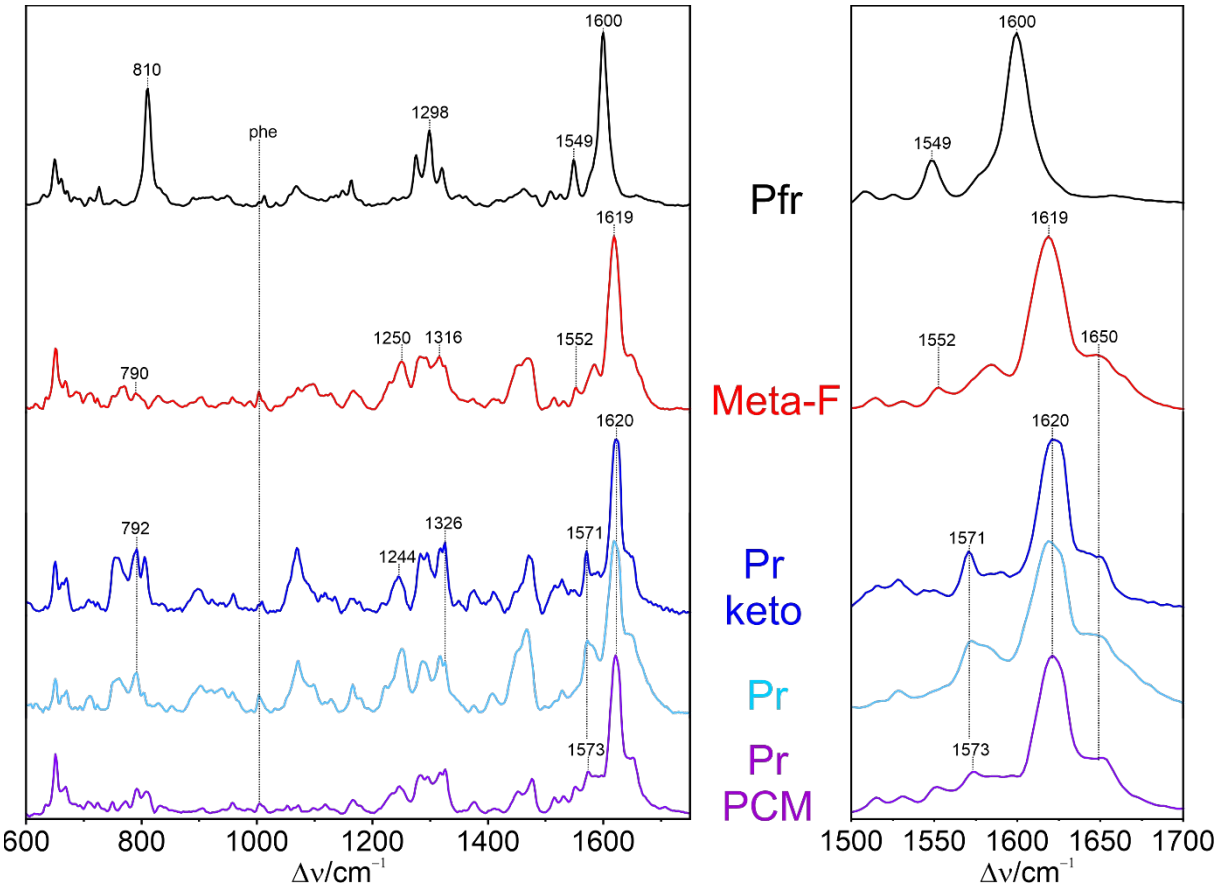

Figure S1. RR spectra of Pfr (black), Meta-F (red), and Pr (light blue) of Agp2-FL. The Pr forms a pH-dependent keto-enol equilibrium with an apparent pK_A of ca. 7.5.[1] Due to the distinctly smaller RR cross section of the enol form, the keto form of Pr prevails at pH 7.8. The pure spectrum of the keto tautomer is represented by the dark blue trace.[1] For a comparison, also the RR spectrum of the Pr state of Agp2-PCM (magenta) is shown. Minor differences compared to that of the full-length variant partly result from the slightly different enol contribution and possible subtraction artifacts since, due to the fast back reaction to Pfr, the spectral contribution of Pr in the raw spectrum was only less than 15%. The dotted vertical line denotes the band of the phenylalanine breathing modes of the apoprotein which was used as an internal standard for evaluation the relative RR cross sections.

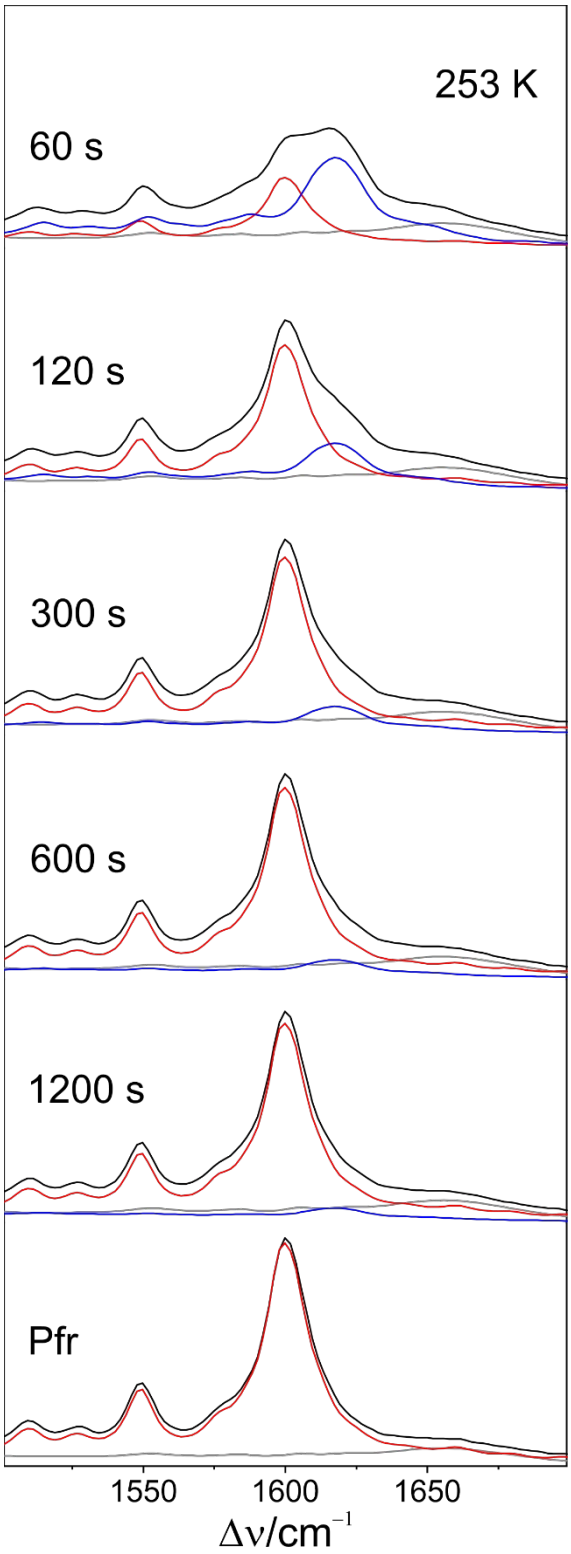

Figure S2. RR spectra of Agp2-FL measured at 90 K after irradiation the sample with 785 nm at 253 K for 60 s (t_{irr}) and keeping the sample in the dark at different times δ, corresponding to total relaxation times of t_{irr}+δ (indicated in the figure). The red, blue, and gray traces refer to the component spectra of Pfr, Meta-F, and the apoprotein, respectively.

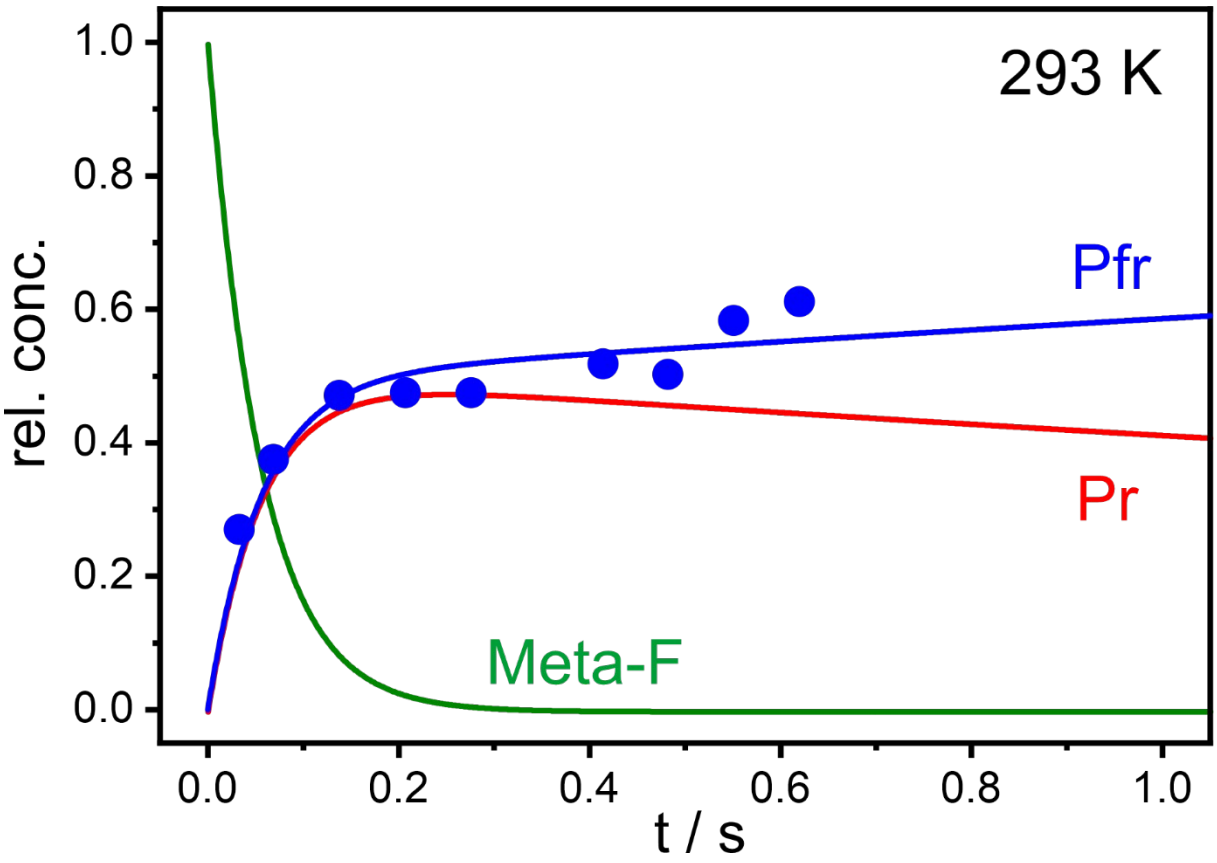

Figure S3. Recovery of the Pfr state of Agp2-PCM following the photoinduced formation of Meta-F. The experimental data (blue symbols) were taken from previous pump-probe time-resolved RR experiments (293 K).[2] The solid lines represent the simulation of the temporal evolution of the Pfr (blue), Meta-F (green), and Pr state (red) according to the kinetic model discussed in the text.

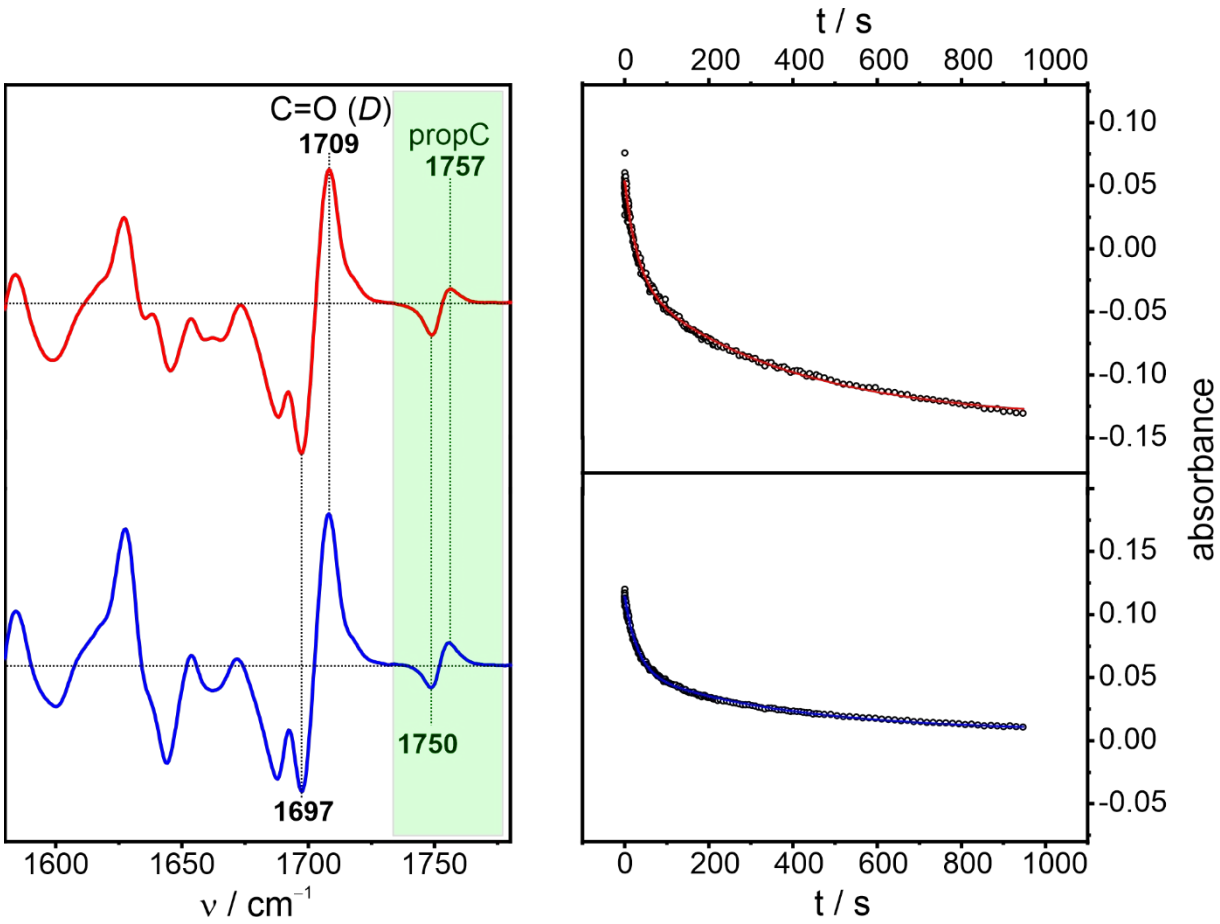

Figure S4. SVD and global fit analysis of the data sets of rapid scan IR difference spectra of Agp2-FL measured at 253 K. The component spectra are shown in the left panel whereas the right panel presents the global fits to the temporal evolution of the first (red) and second component (blue). The green-shaded region marks the C=O stretching of the protonated prop*C*.

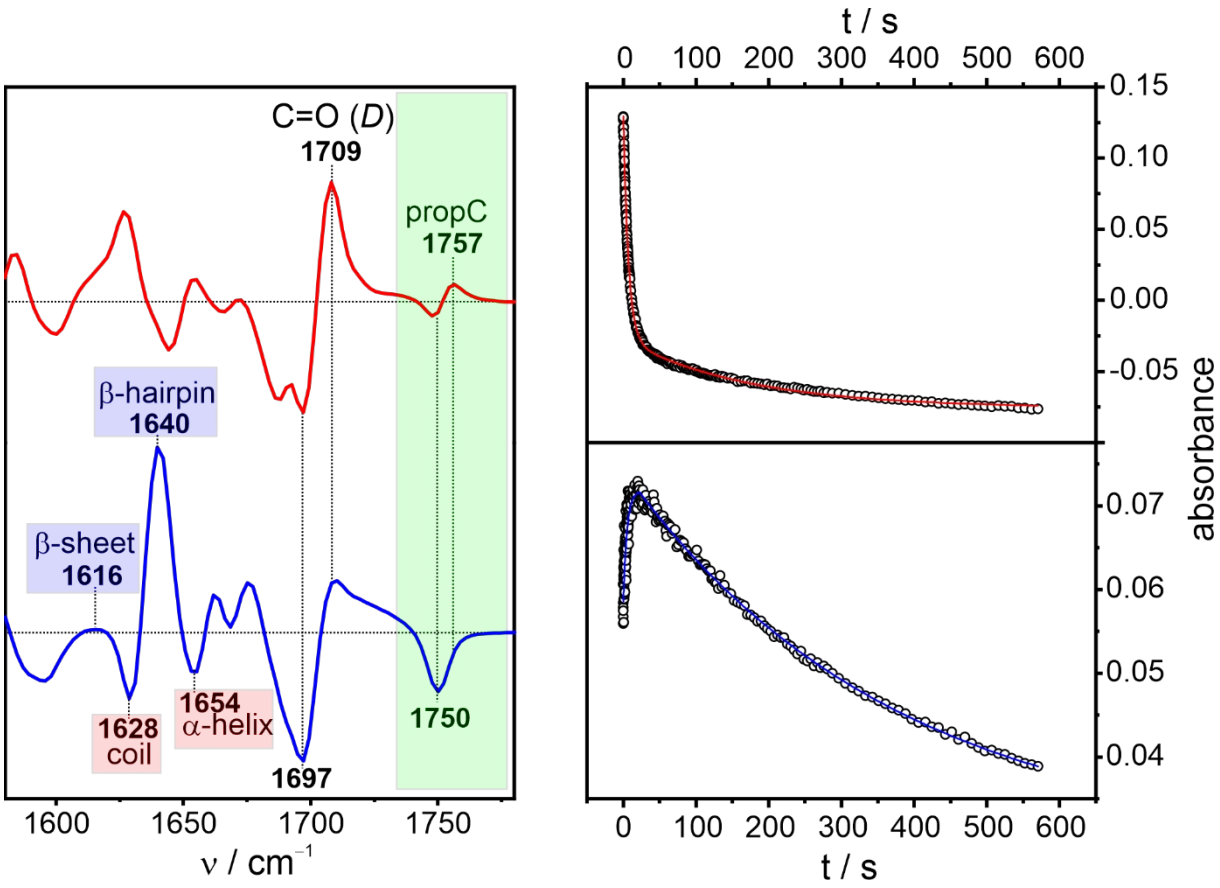

Figure S5. SVD and global fit analysis of the data sets of rapid scan IR difference spectra of Agp2-FL measured at 263 K. The component spectra are shown in the left panel whereas the right panel presents the global fits to the temporal evolution of the first (red) and second component (blue). The green-shaded region marks the C=O stretching of the protonated prop*C*. The signals reflecting the secondary structure change of the tongue are highlighted by the blue- and red-shaded areas.

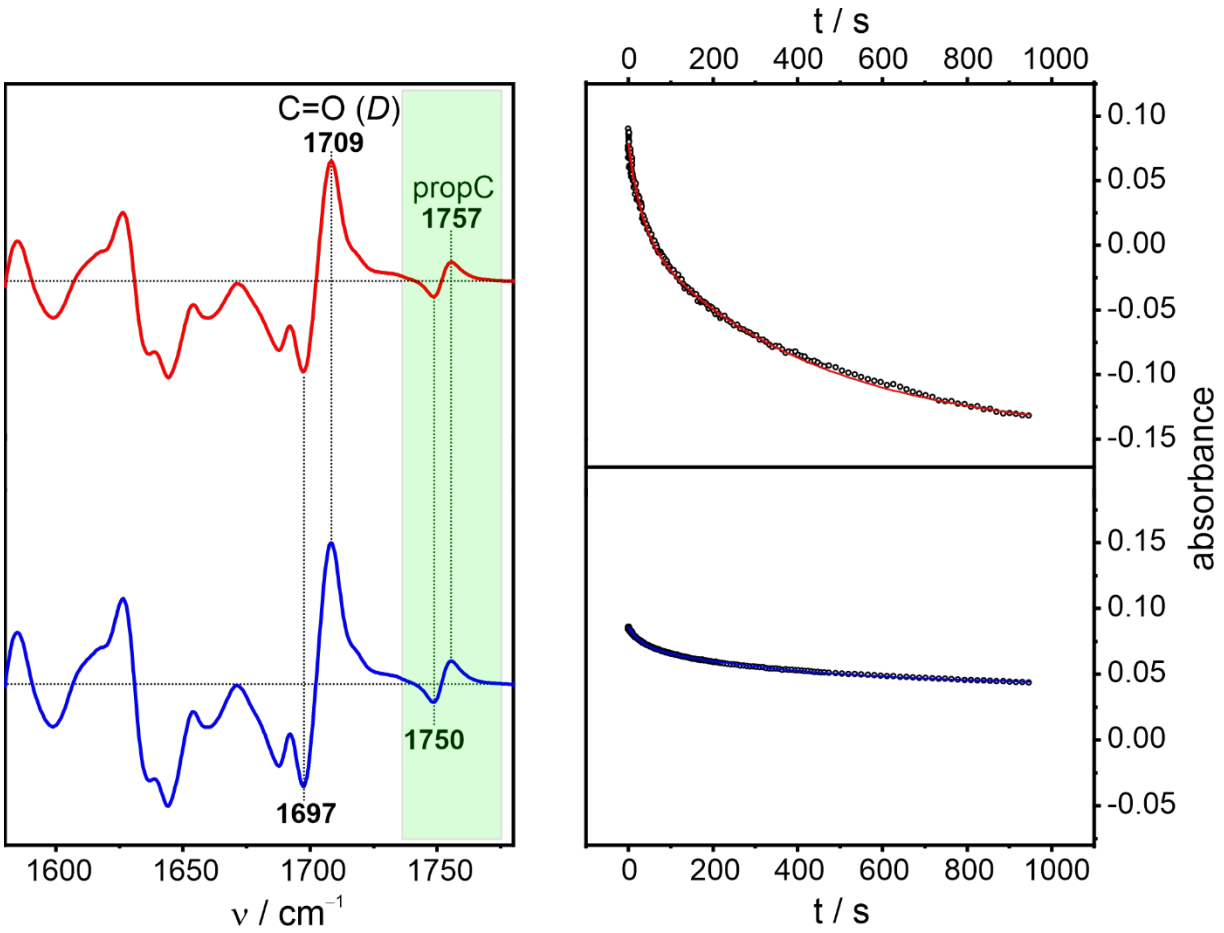

Figure S6. SVD and global fit analysis of the data sets of rapid scan IR difference spectra of Agp2-PCM measured at 243 K. The component spectra are shown in the left panel whereas the right panel presents the global fits to the temporal evolution of the first (red) and second component (blue). The green-shaded region marks the C=O stretching of the protonated prop*C*.

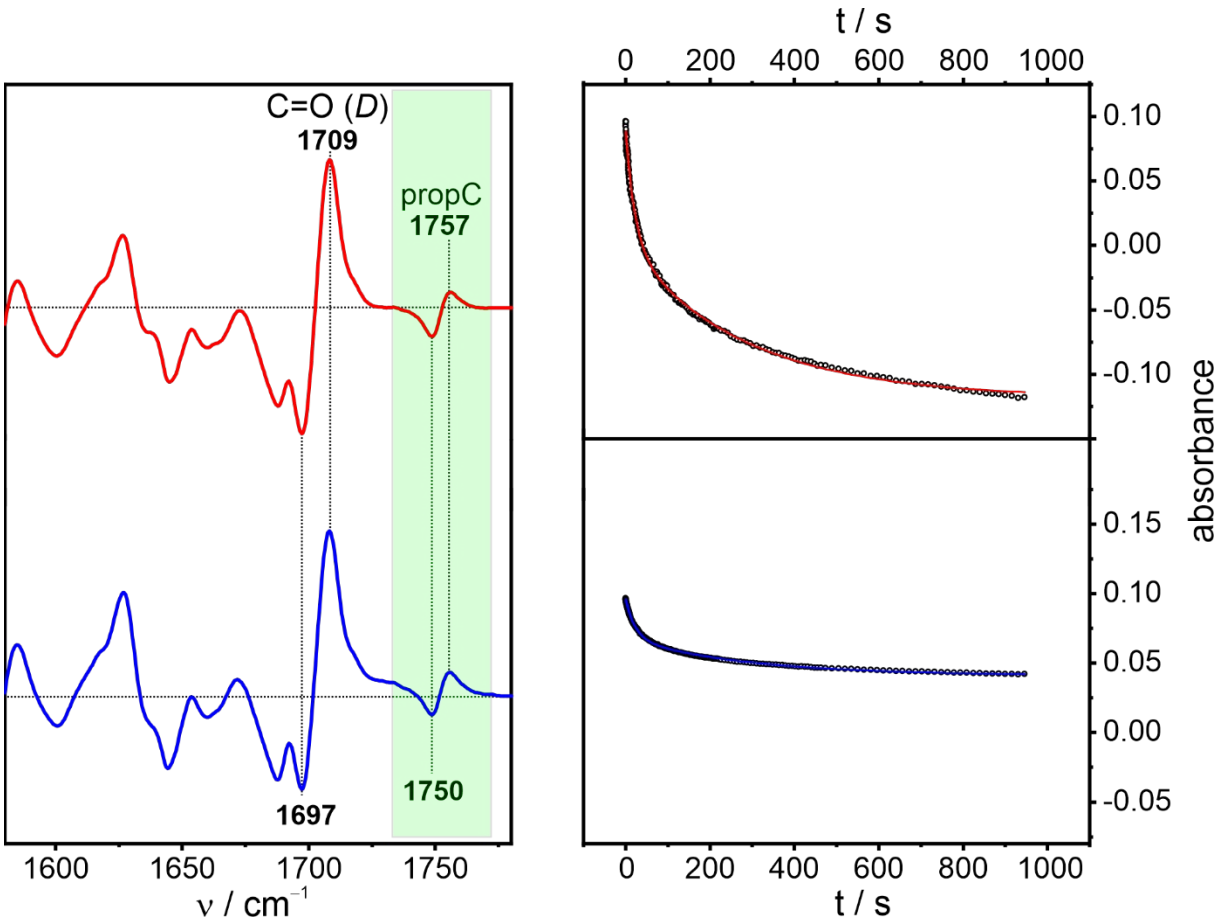

Figure S7. SVD and global fit analysis of the data sets of rapid scan IR difference spectra of Agp2-PCM measured at 253 K. The component spectra are shown in the left panel whereas the right panel presents the global fits to the temporal evolution of the first (red) and second component (blue). The green-shaded region marks the C=O stretching of the protonated prop*C*.

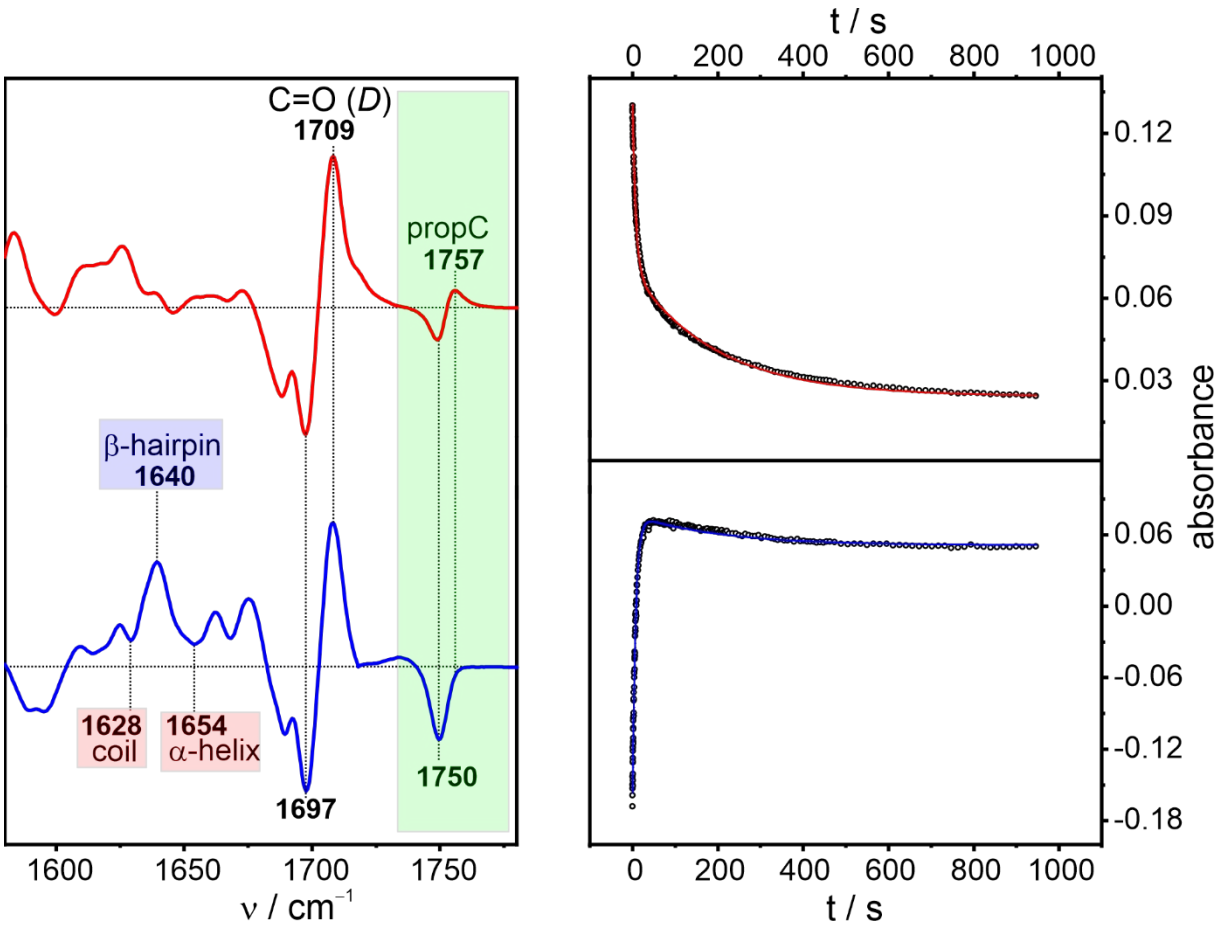

Figure S8. SVD and global fit analysis of the data sets of rapid scan IR difference spectra of Agp2-PCM measured at 263 K. The component spectra are shown in the left panel whereas the right panel presents the global fits to the temporal evolution of the first (red) and second component (blue). The green-shaded region marks the C=O stretching of the protonated prop*C*. The signals reflecting the secondary structure change of the tongue are highlighted by the blue- and red-shaded areas.

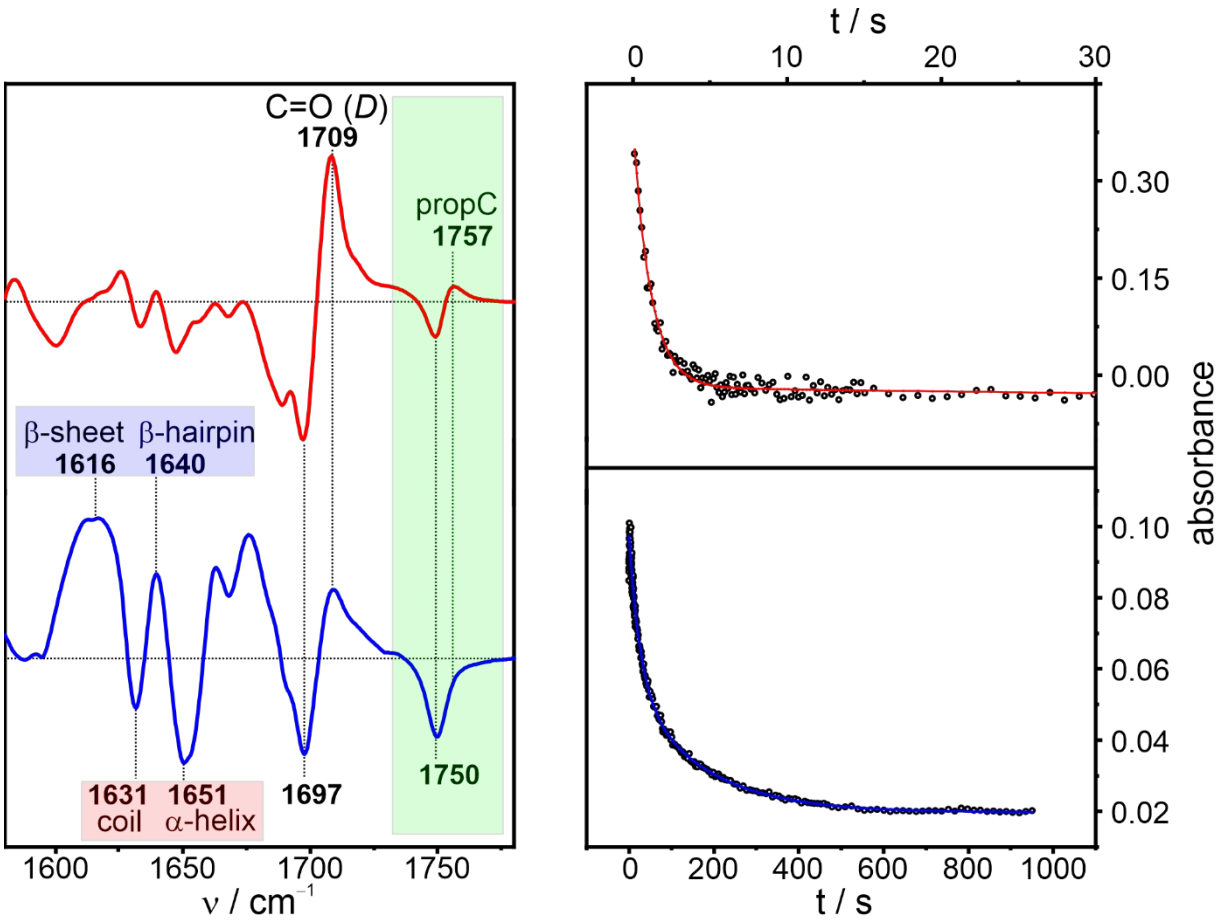

Figure S9. SVD and global fit analysis of the data sets of rapid scan IR difference spectra of Agp2-FL measured at 283 K. The component spectra are shown in the left panel whereas the right panel presents the global fits to the temporal evolution of the first (red) and second component (blue). The green-shaded region marks the C=O stretching of the protonated prop*C*. The signals reflecting the secondary structure change of the tongue are highlighted by the blue- and red-shaded areas.

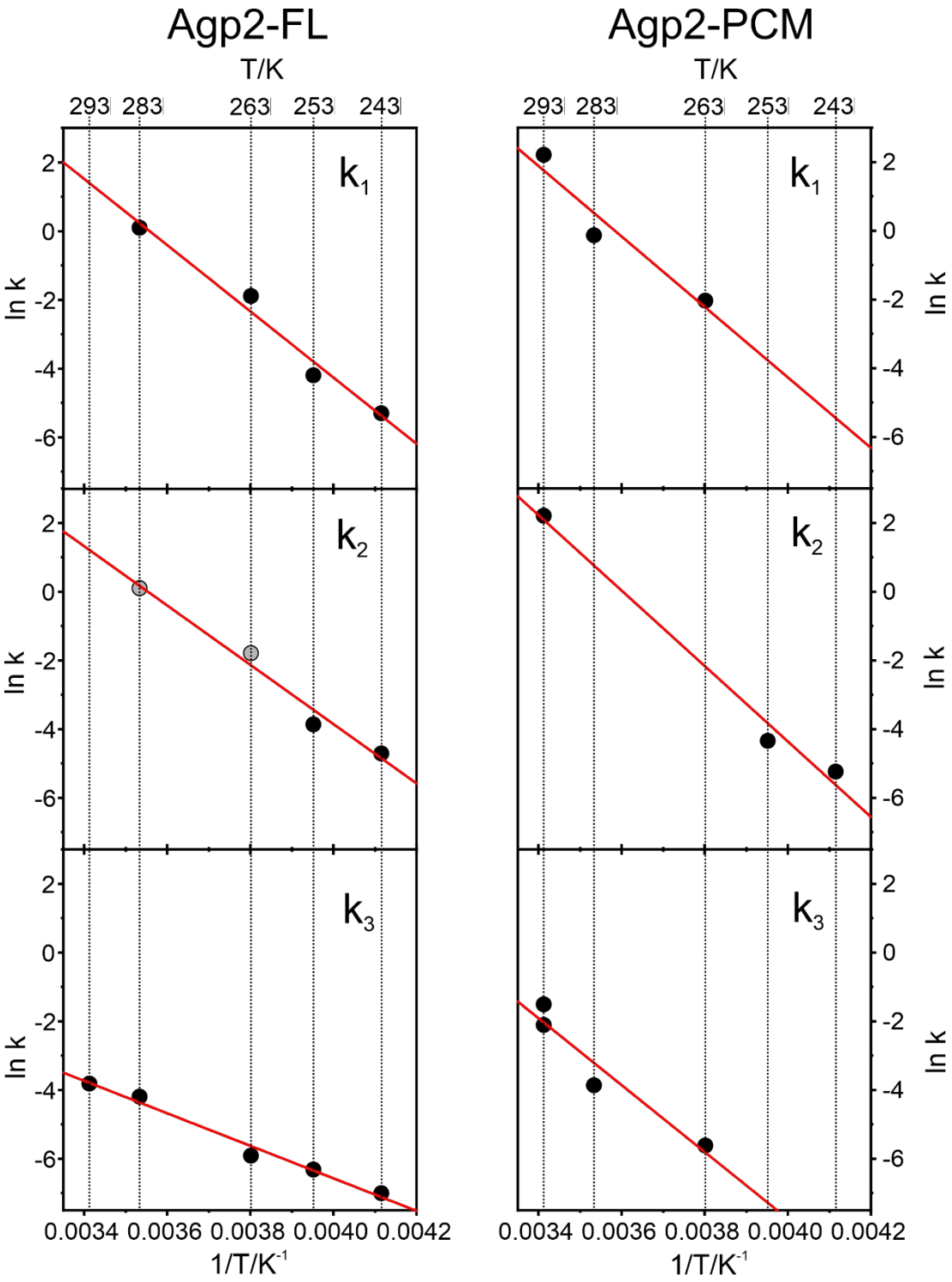

Figure S10. Arrhenius plots (red) of the rate constants of Agp2-FL and Agp2-PCM derived from the spectroscopic experiments (black circles). Note that the gray circles in the plot for k_2 of Agp2-FL are lower limits of the true values. The corresponding activation energies are listed in Table 1.

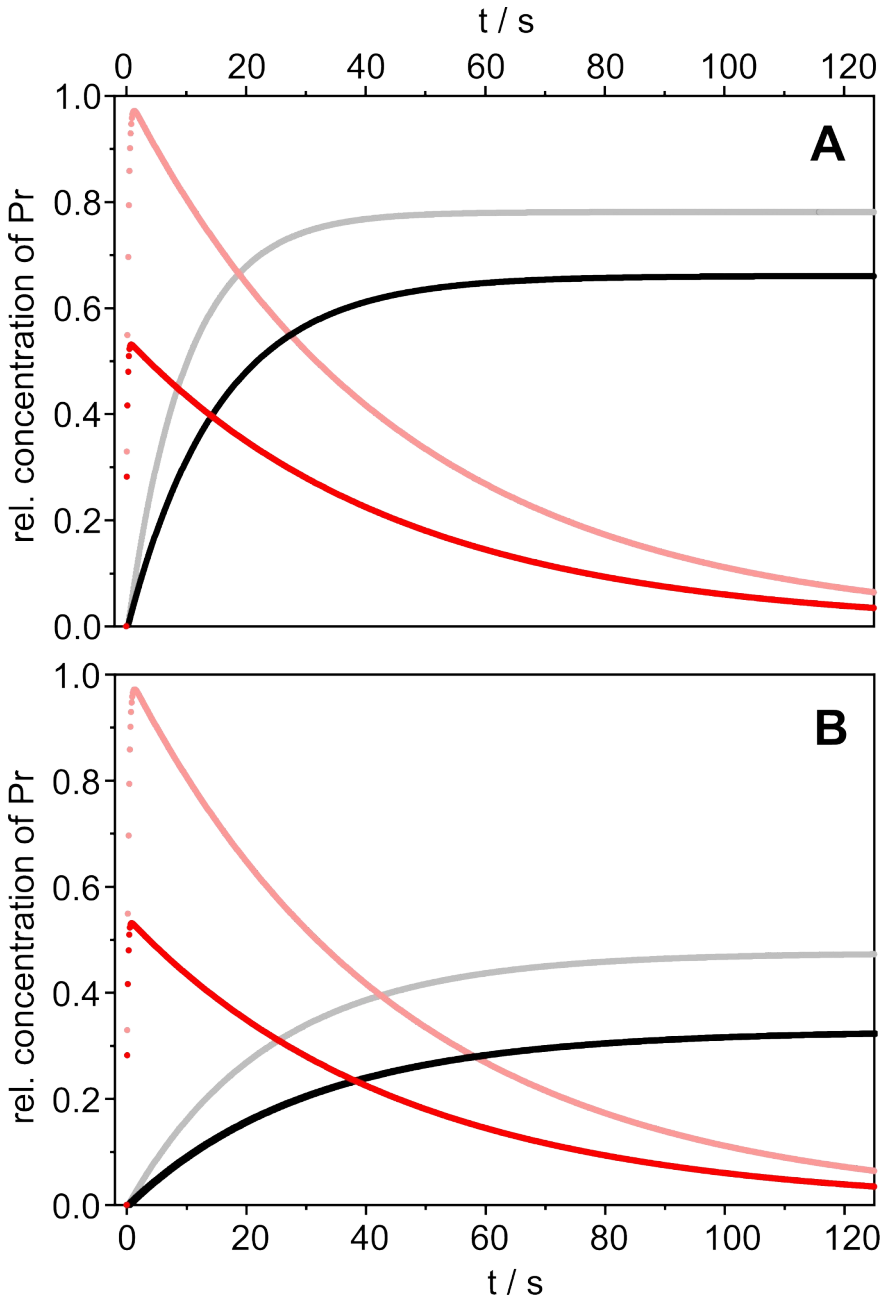

Figure S11. Simulation of the temporal evolution of Pr of Agp2-FL during a period of 125 s. The simulation is based on k_1 = 4 s^{-1}, k_2 = 3.2 s^{-1}, and k_3 = 0.022 s^{-1}, as defined in Figure 5. The values were taken from the Arrhenius plots of the experimental data, extrapolated to 293 K. The red data points describe the situation in which the entire sample is converted to Meta-F at t = 0 s and are identical in A an B (single pulse irradiation). Thus, these curves refer to those experiments in which the irradiation source is switched off after a short but efficient conversion of Pfr to Meta-F (case A, see below). The black data points refer to steady state conditions and thus continuous irradiation (case B, see below) corresponding to an effective

photochemical rate constant k_0 for the Pfr to Meta-F conversion that is four times higher in A (k_0 = 0.08 s^{-1}) than in B (k_0 = 0.02 s^{-1}). The grey and faint red data points refer to continuous and single pulse irradiation but neglecting the direct Meta-F to Pfr decay (k_2 = 0).

A. Single-pulse irradiation

In this case we assume that within a single light pulse Agp2 is converted to Meta-F (relative concentration is set to 1.0) and the decay to Pr (k_1) and subsequently from Pr to Pfr (k_3) as well as the direct decay from Meta-F to Pfr (k_2) can be readily solved to yield the following expressions

(A1) $$[Pfr](t)=1-\frac{k_2-k_3}{k_1+k_2-k_3}\exp\left(-\left(k_1+k_2\right)t\right)-\frac{k_1}{k_1+k_2-k_3}\exp\left(-k_3t\right)$$

(A2) $$[Meta-F](t)=\exp\left(-\left(k_1+k_2\right)t\right)$$

(A3) $$[Pr](t)=1-[Meta-F](t)-[Pfr](t)$$

B. Continuous irradiation

Under these conditions we assume a photochemical rate constant k_0 to describe the conversion from Pfr to Meta-F. The decay of Meta-F is faster than the formation such that the steady state approximation for Meta-F can be employed. Accordingly, we obtain

(B1) $$[Pfr](t)=\frac{k_3}{\lambda}+(1-\frac{k_3}{\lambda})\exp(-\lambda t)$$

with

(B2) $$\lambda=\frac{(k_0+k_3)(k_1+k_2)+k_0(k_3-k_2)}{k_1+k_2}$$

(B3) $$[Meta-F](t)=[Pfr](t)\frac{k_0}{k_1+k_2}$$

(B4) $$[Pr](t)=1-[Pfr](t)-[Meta-F](t)$$

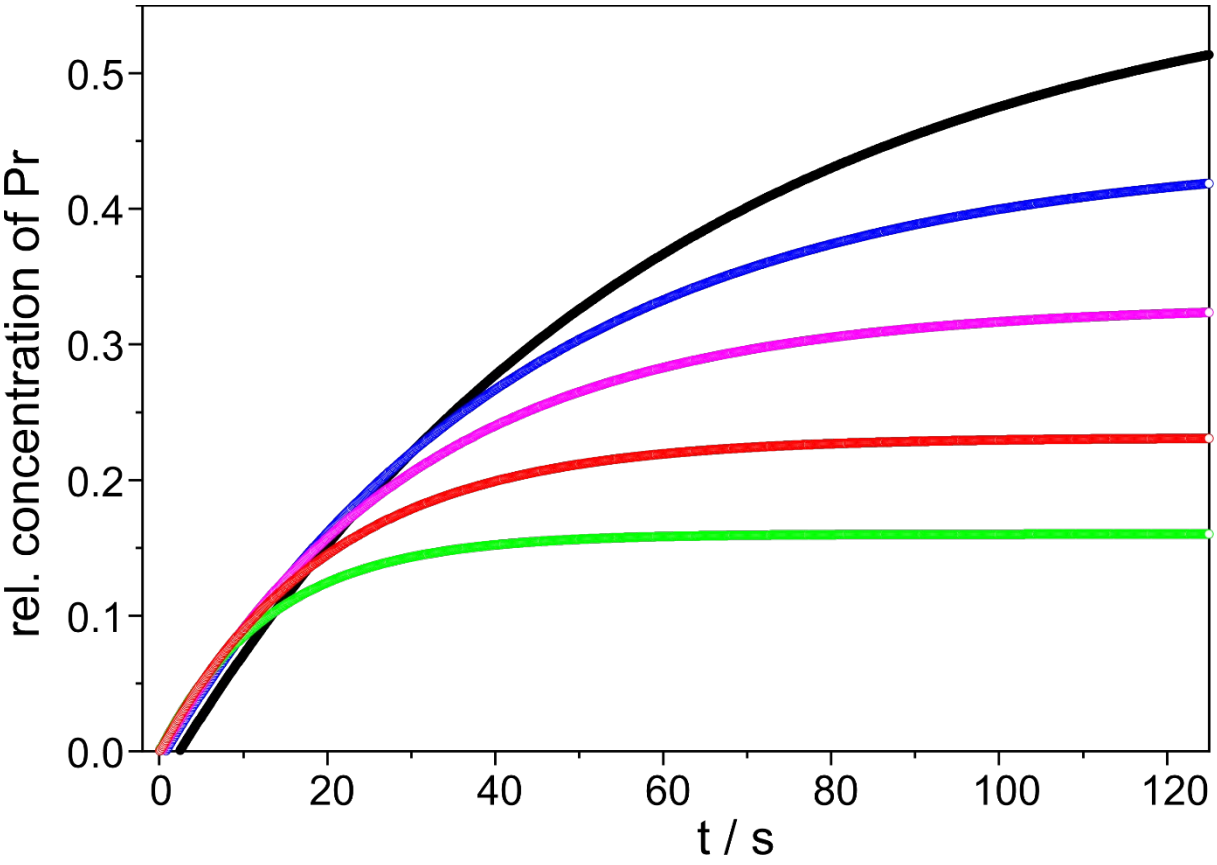

Figure S12. Simulation of the temporal evolution of Pr of Agp2-FL during a period of 125 s under photostationary conditions (as in Figure S10, black curve; $k_0 = 0.04\ s^{-1}$). The simulation is based on values for the rate constants k_1, k_2, and k_3 (defined in Figure 5) taken from the Arrhenius plots of the experimental data (Fig. S10) but extrapolated to 273 K (black), 283 (blue), 293 K (magenta), 303 K (red), and 313 K (green).

References

1 F. Velazquez Escobar, P. Piwowarski, J. Salewski, N. Michael, M. Fernandez Lopez, A. Rupp, M. B. Qureshi, P. Scheerer, F. Bartl, N. Frankenberg-Dinkel, F. Siebert, M. A. Mroginski and P. Hildebrandt, A protonation-coupled feedback mechanism controls the signalling process in bathy phytochromes, *Nat. Chem.*, 2015, **7**, 423–430.

2 D. Buhrke, U. Kuhlmann, N. Michael and P. Hildebrandt, The Photoconversion of Phytochrome Includes an Unproductive Shunt Reaction Pathway, *ChemPhysChem*, 2018, **19**, 566–570.